

Article

Benzene, an Unexpected Binding Unit in Anion– π Recognition: The Critical Role of CH/ π Interactions

 David Quiñonero * and Antonio Frontera 

Department of Chemistry, Universitat de les Illes Balears, Crta. de Valldemossa km 7.5, 07122 Palma de Mallorca, Spain

* Correspondence: david.quinonero@uib.es

Abstract: We report high-level ab initio calculations (CCSD(T)(full)/CBS//SCS-RI-MP2(full)/aug-cc-pwCVTZ) that demonstrate the importance of cooperativity effects when Anion– π and CH/ π interactions are simultaneously established with benzene as the π -system. In fact, most of the complexes exhibit high cooperativity energies that range from 17% to 25.3% of the total interaction energy, which is indicative of the strong influence of the CH/ π on the Anion– π interaction and vice versa. Moreover, the symmetry-adapted perturbation theory (SAPT) partition scheme was used to study the different energy contributions to the interaction energies and to investigate the physical nature of the interplay between both interactions. Furthermore, the Atoms in Molecules (AIM) theory and the Non-Covalent Interaction (NCI) approach were used to analyze the two interactions further. Finally, a few examples from the Protein Data Bank (PDB) are shown. All results stress that the concurrent formation of both interactions may play an important role in biological systems due to the ubiquity of CH bonds, phenyl rings, and anions in biomolecules.

Keywords: Anion– π interactions; CH/ π interactions; cooperativity



Citation: Quiñonero, D.; Frontera, A. Benzene, an Unexpected Binding Unit in Anion– π Recognition: The Critical Role of CH/ π Interactions. *Sci* **2022**, *4*, 32. <https://doi.org/10.3390/sci4030032>

Academic Editors: Sławomir Grabowski and Maxim L. Kuznetsov

Received: 11 May 2022

Accepted: 17 August 2022

Published: 22 August 2022

Publisher's Note: MDPI stays neutral with regard to jurisdictional claims in published maps and institutional affiliations.



Copyright: © 2022 by the authors. Licensee MDPI, Basel, Switzerland. This article is an open access article distributed under the terms and conditions of the Creative Commons Attribution (CC BY) license (<https://creativecommons.org/licenses/by/4.0/>).

1. Introduction

Comprehension of non-covalent interactions lays the foundation of the interdisciplinary field of supramolecular chemistry. In particular, interactions with aromatic rings play a vital role in a great deal of chemical and biological processes, such as molecular recognition, crystal engineering, and conformational changes [1].

Anion– π interactions are a prominent type of attractive non-covalent force that was put in the spotlight of the scientific community from the pioneering computational studies that first appeared back in 2002 [2–5], igniting great interest in further analyzing the nature and quantification of these interactions from both theoretical and experimental points of view [6]. Since then, many theoretical studies have been reported focusing on this type of interaction [7–11]. In fact, several reviews of these studies have appeared in the literature [12–18], converting Anion– π interactions into a live topic nowadays. For instance, very recently, *i*-corona[3]arene[3]tetrazines have been reported to regulate their macrocyclic conformation and cavity structures to recognize anions by forming interdependent and synergistic Anion– π /and hydrogen bond interactions [19]. In another recent study, Anion– π interactions of azacalix[3]triazines alter their ionization potentials and capture protons as organic superbases, despite the electron-deficient nature of triazine [20]. Another very recent study reports a series of rotaxane-based Anion– π catalysts in which the mechanical bond between a bipyridine macrocycle and an axle containing a naphthalene diimide unit that catalyses an otherwise disfavoured Michael addition in >60 fold selectivity over a competing decarboxylation pathway [21].

In Anion– π complexes, the π system is usually an electron-deficient arene and, thus, the interaction is often dominated by electrostatic due to its positive quadrupole moment and ion-induced polarization terms [2–4,8,9]. Therefore, from an electrostatic perspective,

the interaction of benzene, with a negative quadrupole moment with anions is counterintuitive since it would result in a repulsive Coulombic interaction. However, several theoretical studies have appeared in the literature showing that the interaction between electron-rich aromatic systems and anions is feasible. For instance, Lewis et al. showed that negative quadrupole aromatics, such as benzene and several of its halo derivatives, bind fluoride through Anion- π interactions [22]. In another report, electron-rich alkyl/alkenyl/alkynyl-substituted benzenes and triphenylene were shown to favorably interact with halides [23]. Very recently, the presence of favourable Anion- π interactions between chlorine oxyanions and the π -system of the unsubstituted benzene ring was demonstrated [24]. The first theoretical and experimental evidence of an Anion- π interaction of an electron-rich alkylbenzene ring was reported several years ago. Here, the cyclophane cavity, bridged with three naphthoimidazolium groups, is found to selectively capture fluoride by means of Anion- π interactions and ionic hydrogen bonds [25].

Anion- π interactions have also been the object of study in biomolecular systems. The crucial role of this non-covalent interaction was reported for the first time in 2011 when our group reported strong evidence of the inhibition of the enzymatic activity caused by Anion- π interactions [26]. In the same year, three additional studies appeared indicating the importance of these interactions in protein structures [27–29]. Other studies pointed out that Anion- π interactions unambiguously play an important role in macromolecular folding and function in proteins and nucleic acids [30] and the structural stability of the Sm/LSm proteins [31]. Our group has also reported the critical role of Anion- π interactions in the mechanism of sulfide: quinone oxidoreductase [32] and in the mechanism of inhibition of phenyldiketo acids of malate synthase [33]. Protein Data Bank (PDB) searches have also been carried out, focusing on interactions between phenylalanine (Phe) and negatively charged residues such as aspartate (Asp) and glutamate (Glu), concluding their presence in thousands of protein structures [29,34]. In particular, it has been shown that anionic Asp can interact favourably with Phe to strongly stabilize the WW domain (a well-characterized β -sheet model system) of the human protein Pin 1 by -1.3 kcal/mol [35].

Another non-covalent and relatively recent type of force is the CH/ π interaction [36–38]. Despite its weakness (for the methane-benzene complex, the binding energy in the gas phase was calculated to be -1.5 kcal/mol) [39], it is shown to be crucial as the driving force in crystal packing [36], host-guest chemistry [40], conformation [41–43], and reaction selectivity [44] of organic compounds. For instance, Davis et al. developed cage-type host systems for the selective recognition of cellobiose, where CH/ π interactions are key to the formation of stable 1:1 complexes [45,46]. In other studies, Rebek et al. found that CH/ π interactions are responsible for the stabilization of complexes where long-chain alkanes are enclosed in the confined space of cavitands [47,48]. Self-assembled capsules [49,50] CH/ π interactions have also been reported to participate, as the major discriminating force, in the diastereoselectivity between diastereoisomeric complexes in aminoacid derivatives [51] and methylmethanetriacetic acid recognition [52,53]. The CH/ π interaction is dominated by the dispersion contribution and the electrostatic term is small [54,55], unlike conventional hydrogen bonds where the coulombic interaction is the major contributor [56].

Moreover, due to the omnipresence of both alkyl and phenyl groups in biomolecules, much evidence for the CH/ π interaction in biological systems has been reported [57]. In fact, CH/ π interaction plays an important role in stabilizing the three-dimensional structure of proteins and their complexes [58–62]. All these findings support the thesis that this interaction is essential for a deeper understanding of molecular biology [36,57].

Anion- π interactions are also very frequent in biological systems, with more than half of the biomolecular complexes of the protein data bank containing at least one Anion- π contact, i.e., one Anion- π interaction for every 50 anionic residues in the PDB [63]. Moreover, thousands of the arene moieties engaged in Anion- π interactions are also found to be involved in cation- π and π -stacking interactions on the opposite side of the aromatic ring, a fact that may lead to cooperativity effects [64].

Recently, we and others reported theoretical and experimental evidence for cooperativity effects in complexes in which different interactions coexist, namely, Anion- π and π - π stacking [64,65], Anion- π and hydrogen-bonding interactions [66–69], Anion- π and Ar/ π [70], Anion- π and halogen-bonding interactions [71–73] and Anion- π and triel bond interactions [74]. It has been found that such interplays can lead to strong cooperativity effects. In this manuscript, we present a computational study using high-level ab initio calculations (CCSD(T)(full)/CBS//SCS-RI-MP2(full)/aug-cc-pwCVTZ) in which we address cooperativity effects between CH/ π $\alpha\gamma\delta$ Anion- π interactions and analyze their importance in biological systems due to the ubiquity of CH bonds (as in methyl groups), phenyl rings (as in the side chains in Phe and Tyr) and anions (as in Asp and Glu). We selected the benzene molecule as a model of phenyl moieties, the methane molecule as a model of an alkyl chain, and formate and nitrate anions as models for carboxylate anions. We first computed the geometric and energetic features of the CH/ π complexes 1–3 and Anion- π complexes 4–7. Secondly, we calculated CH/ π -anion complexes 8–11 to study cooperativity effects between both types of interactions, viz., how the Anion- π interaction is affected by the CH/ π interaction and vice versa. Moreover, the symmetry-adapted perturbation theory (SAPT) energy partitioning scheme was used to investigate the different energy contributions to the interactions energies and to examine the physical nature of the interplay between both interactions. Finally, the Atoms in Molecules (AIM) theory and the Non-Covalent Interaction (NCI) approach were used to further analyze the two interactions. To the best of our knowledge, no computational studies have been reported on the study of the interaction between either carboxylate or nitrate anions with benzene.

2. Computational Details

The geometry of the compounds under study was optimized using the resolution of the identity MP2 (RI-MP2) [75,76], with all electrons correlated and imposing the highest group symmetry for each case. In addition, the spin-component scaled MP2 method (SCS-RI-MP2) has been used [77,78]. The SCS-RI-MP2 correlation treatment yields better structures than the standard MP2, especially in systems dominated by dispersion effects [79]. The calculations were carried out using Dunning's correlation-consistent polarized weighted-core valence basis sets of triple- ζ (aug-cc-pwCVTZ, abbreviated as AVTZ). Furthermore, we used a truncated AVTZ basis, denoted AVTZ', which removes diffuse functions from the hydrogen atoms not involved in hydrogen bonding.

The energies of the compounds were improved by using the CCSD(T)/CBS level of theory [80]. The CCSD(T) method provides reliable interaction energies only when brought together with extended atomic orbitals basis sets. It is recommended that the relevant calculations be performed at the complete basis-set (CBS) limit. The extrapolation scheme of Helgaker et al. [81,82] has become the most widely used. Here, the HF and MP2 energies are separately extrapolated as follows:

$$E_X^{\text{HF}} = E_{\text{CBS}}^{\text{HF}} + Ae^{-\alpha X} \quad (1)$$

$$E_X^{\text{MP2}} = E_{\text{CBS}}^{\text{MP2}} + BX^{-3} \quad (2)$$

$$E_X^{\text{MP2}} = E_{\text{CBS}}^{\text{MP2}} + BX^{-3} \quad (3)$$

where E_{CBS} and E_X are the energies for the complete basis set and for the basis set with the largest angular momentum X , respectively. The CCSD(T)/CBS level can be achieved following an extrapolation of the MP2 and higher-order correlation energies towards the basis-set limit (equation 3). In this case, each of the components shows different sensitivity to the atomic orbital basis set: the MP2 correlation energy is the one that converges more slowly, and the larger the basis set used in the extrapolation, the better. In our manuscript, we used a two-point extrapolation scheme using the AVTZ and the aug-cc-pVQZ basis sets. The third term, called the CCSD(T) correction term ($\Delta E^{\text{CCSD(T)}} - \Delta E^{\text{MP2}}$), converges much faster than the MP2 correlation energy and is obtained as the difference between the CCSD(T) and MP2 energies. In our case, we have used the AVTZ' basis set to

calculate the CCSD(T) correction. All the geometry optimizations were performed by using TURBOMOLE version 7.0 [83], and CBS calculations were carried out with the help of the MOLPRO program [84].

The interaction energies were determined as the difference between the energy of the complex and the energies of the optimized isolated monomers.

In complexes in which CH/ π and an Anion- π interactions coexist, we computed the cooperativity energy E_{coop} using Equation (4)

$$E_{\text{coop}} = E(\text{H}\pi + \text{A}\pi) - E(\text{H}\pi) - E(\text{A}\pi) - E(\text{HA}) \quad (4)$$

where $E(\text{H}\pi)$ and $E(\text{A}\pi)$ and $E(\text{H}\pi + \text{A}\pi)$ terms correspond to the interaction energies of the corresponding optimized two-component CH/ π and Anion- π complexes and the three-component CH/ π -anion complexes, respectively, and $E(\text{HA})$ is the interaction between methane and the anion in the CH/ π -anion complexes. This equation has been successfully used to investigate cooperativity effects when two different interactions coexist in a variety of systems, namely π systems as simultaneous hydride- and hydrogen-bond acceptors, the concurrent interaction of tetrafluoroethylene with anions and hydrogen-bond donors [66,67], Anion- π and halogen-bonding interactions [71], and ion- π and Argon/ π interactions [68].

The bonding features were studied by using the Atoms-in-Molecules (AIM) theory [85,86]. For this purpose, we have found the most relevant bond and cage critical points (BCP and CCP, respectively) and evaluated the electron density at each CP with the help of the AIMAll program package [87].

The SAPT (Symmetry Adapted Perturbation Theory) [88] method permits the decomposition of the interaction energy into different contributions related to physically well-defined components, such as those arising from induction, electrostatic, dispersion, and exchange terms. Within the framework of the SAPT method, the interaction energy can be expressed as [89]:

$$E_{\text{int}} = E_{\text{el}} + E_{\text{exch}} + E_{\text{ind}} + E_{\text{disp}} \quad (5)$$

where E_{el} is the electrostatic interaction energy of the monomers; E_{exch} is the first-order exchange energy term; E_{ind} represents the second-order induction energy; E_{disp} is the second-order dispersion energy.

The density fitting DFT-SAPT (DF-DFT-SAPT) method has been utilized to analyze the interaction energies of the complexes. In this method, the energies of interacting monomers are expressed in terms of orbital energies obtained from the Kohn-Sham density functional theory [90,91]. Besides the terms listed in Equation (5), a Hartree-Fock correction term δHF , which accounts for third- and higher-order induction and exchange corrections, has been included [92]. The DF-DFT-SAPT calculations have been carried out by using the PBE0/aug-cc-pVQZ/aug-cc-pwCVTZ-PP computational method [93]. The JK-fitting basis of Weigend [94] was used as an auxiliary fitting basis set. The cc-pV5Z JK-fitting basis was employed for all atoms. For the intermolecular correlation terms, i.e., the dispersion and exchange-dispersion terms, the related aug-cc-pVQZ MP2-fitting basis of Weigend, Köhn, and Hättig [95] were employed. All SAPT calculations have been performed with the MOLPRO program [84].

To further characterize CH/ π and Anion- π interactions in real space based on the electron density, the noncovalent interaction NCI analysis based on the reduced density gradient (RDG) method [96] has been performed using the AIMAll program package [87].

3. Results and Discussion

3.1. Energetic and Geometric Details of CH/ π and Anion- π Complexes

Table 1 and Figure 1 summarize the binding energies and equilibrium distances of complexes 1–7. First, we will address the CH/ π complexes 1–3. The interaction energies of complexes between benzene and methane are small and vary from -1.21 to -1.46 kcal/mol depending on the number of CH bonds pointing at the benzene molecular plane. The most

favorable configuration of the benzene-methane complex is found for complex **1**, i.e., the one that only points one CH bond at the ring, with interaction energy of -1.46 kcal/mol, comparable to previously reported results at the CCSD(T)/CBS level of theory [39]. In complexes **2a** and **2b**, the methane molecule points to two CH bonds at the benzene ring either at carbon atoms or at the middle point of CC bonds. The binding energies of **2a** and **2b** are almost the same, -1.37 and -1.38 kcal/mol, respectively, and slightly smaller than the one obtained for **1**. In complexes **3a** and **3b**, the methane molecule positions three hydrogen atoms on the benzene molecule, either pointing at carbon atoms or at the middle point of CC bonds, yielding binding energies of -1.21 and -1.23 kcal/mol, respectively. Therefore, depending on the positioning of the methane molecule, the binding energy for the interaction with benzene will only vary around 0.25 kcal/mol between the most and least favorable configurations, thus confirming the weak orientation dependence of the CH/ π interaction [97]. The equilibrium distance in CH/ π complexes ($R_{H\pi}$, Table 1 and Figure 1), defined as the distance between the carbon atom of the methane molecule and the molecular plane of benzene, ranges from 3.753 Å for complex **1** to 3.634 Å for complexes **3a** and **3b**. Thus, as expected by the similar binding energies, there is a small variation of the equilibrium distances (only 0.119 Å) between the most and least favorable configurations for the CH/ π complexes.

Table 1. Equilibrium distances ($R_{H\pi}$, $R_{A\pi}$, in Å) at the SCS-RI-MP2/AVTZ and interaction energies (E , in kcal/mol) at the CCSD(T)/CBS levels of theory.

Compound	$R_{H\pi}$ [a]	$R_{A\pi}$ [a]	$\Delta R_{H\pi}$ [b]	$\Delta R_{A\pi}$ [b]	E
1	3.753	-	-	-	-1.46
2a	3.673	-	-	-	-1.37
2b	3.675	-	-	-	-1.38
3a	3.634	-	-	-	-1.21
3b	3.634	-	-	-	-1.23
4a	3.931	3.400	-	-	0.01
4b	3.927	3.396	-	-	0.02
5	-	3.200	-	-	0.53
6a	-	3.374	-	-	0.20
6b	-	3.371	-	-	0.20
7a	-	3.376	-	-	-1.02
7b	-	3.372	-	-	-0.99
8a	3.714	3.361	-0.039	-0.035	-2.12
8b	3.714	3.366	-0.039	-0.034	-2.14
9a	3.646	3.369	-0.027	-0.027	-1.90
9b	3.649	3.372	-0.026	-0.028	-1.92
9c	3.644	3.371	-0.029	-0.029	-1.90
9d	3.648	3.367	-0.027	-0.029	-1.90
10a	3.633	3.376	-0.001	-0.020	-1.59
10b	3.634	3.381	0.000	-0.019	-1.62
10c	3.640	3.379	0.006	-0.021	-1.60
10d	3.634	3.378	0.000	-0.018	-1.60
11a	3.709	3.350	-0.046	-0.022	-3.03
11b	3.708	3.352	-0.045	-0.024	-3.05

[a] Equilibrium distances $R_{H\pi}$ and $R_{A\pi}$ from C and O to the ring plane, respectively. [b] The variation of the equilibrium distances with respect to the corresponding binary complexes ($\Delta R_{H\pi}$ and $\Delta R_{A\pi}$, in Å).

Let us continue with the Anion- π complexes, starting with the ones with formate (complexes **4a** and **4b**). Due to symmetry constraints, we have only considered the complexes shown in Figure 1. The binding energies of the carboxylate complexes are tiny and positive (not favorable, Table 1 and Figure 1), as expected from an electrostatic point of view for the interaction of an anion with an electron-rich aromatic system, such as benzene, that exhibits a negative quadrupole moment. The orientation of the formate anion, with both O atoms either pointing at C atoms of benzene or pointing at CC middle bonds, does not have any significant impact on the energetics and geometric features of the anion complexes, as

can be inferred from the data collected in Table 1. For the nitrate- π complexes, we have explored different configurations shown in Figure 1 with one, two, and three of its O atoms pointing at the benzene molecule (complexes 5, 6a–b, and 7a–b, respectively). As expected, the interaction energy for complex 5 is not favorable (0.53 kcal/mol) with an equilibrium distance ($R_{A\pi}$, Table 1 and Figure 1) of 3.200 Å, defined as the distance between the O atom and the molecular plane of benzene. Ongoing from complex 5 to 6a or 6b, the interaction energy becomes less positive (0.20 kcal/mol) with equilibrium distances slightly larger than the one found in complex 5. However, the complexes where all three O atoms of the nitrate anion point at the ring (complexes 7a and 7b) yield favorable configurations with negative interaction energies of -1.02 kcal/mol and -0.99 kcal/mol, depending on the orientation of the anion. Therefore, surprisingly, the interaction of benzene with nitrate is favorable only if the anion is stacked with the aromatic system. In these cases, the equilibrium distances are very similar to the ones found in complexes 6a and 6b. This behavior is likely related to the electrophilic role of the central N-atom of the nitrate anion in these complexes. In fact, it has been demonstrated that nitrate anion can act as an electrophile in the solid state [98].

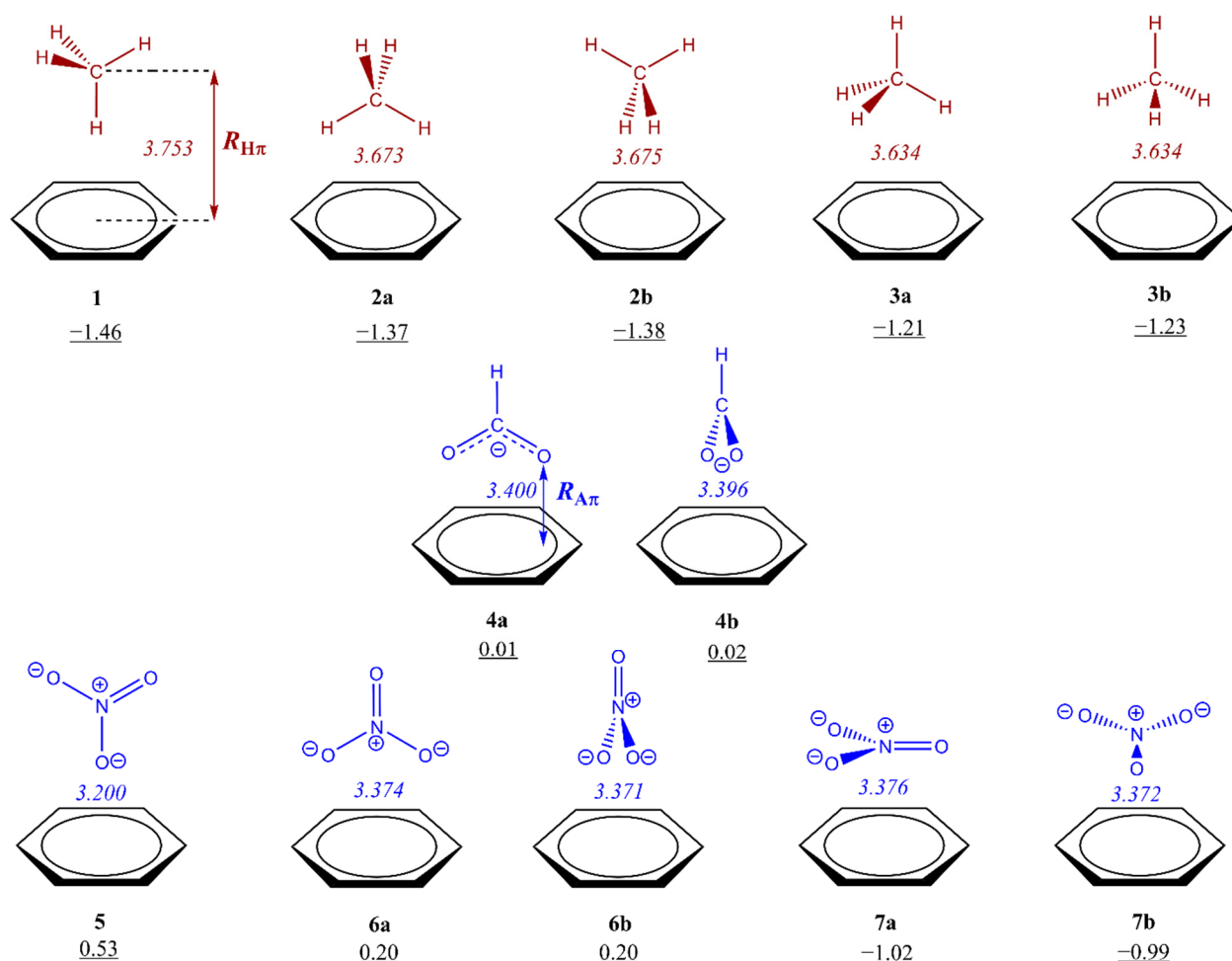


Figure 1. CH/ π (1–3) and Anion- π (4–7) complexes under study. Binding energies (in kcal/mol) are underlined, and equilibrium distances (in Å) are shown in italics.

3.2. Energetic and Geometric Details of Three-Component CH/ π and Anion- π Complexes

The geometric and energetic results computed for multicomponent complexes 8–11 are summarized in Table 1 and Figure 2. We have considered both orientations of formate in the three-component complexes (complexes 8–10). In the case of nitrate, configurations where either one or two O atoms are pointing at the ring, have not been considered in

the three-component complexes under study because we expect they would yield similar results to those of formate complexes. Thus, we have only considered the configurations where nitrate is establishing stacking interactions due to its uniqueness (**11a–b**).

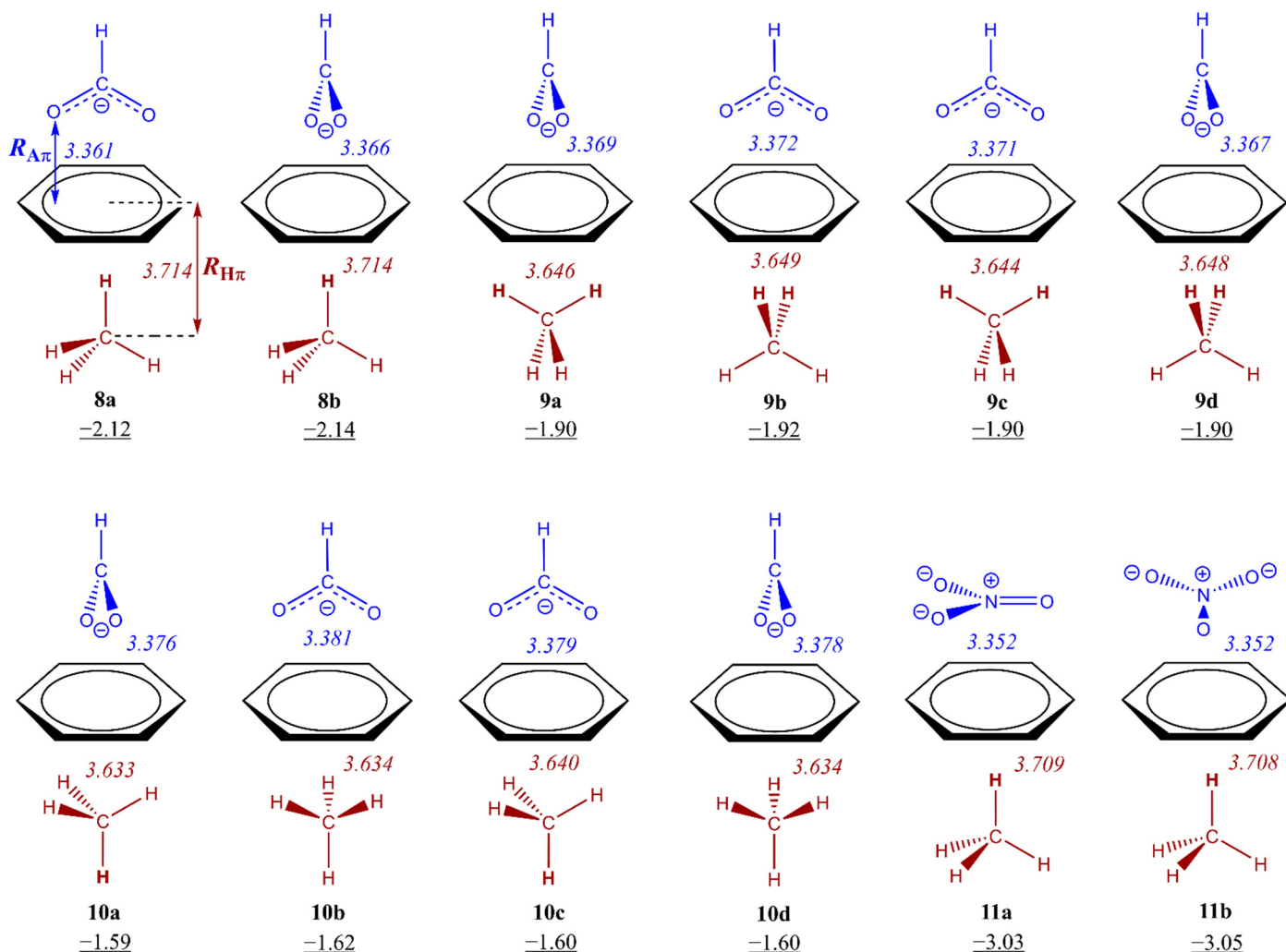


Figure 2. CH/ π -anion complexes (**8–11**) under study. Binding energies (in kcal/mol) are underlined, and equilibrium distances (in Å) are shown in italics.

Some interesting points can be extracted from the geometrical results. In all cases, the equilibrium distance of the Anion- π interactions in CH/ π -anion complexes **8–11** is shorter than in their respective two-component complexes **4–7** (see $\Delta R_{A\pi}$ in Table 1), i.e., the presence of the CH/ π interaction reinforces the Anion- π interactions. Moreover, the equilibrium distance of the CH/ π interaction $R_{H\pi}$ in complexes **8–11** is also shorter compared to complexes **1–3**, i.e., the presence of the Anion- π interactions also reinforces the CH/ π interaction. There are three exceptions, the complexes **10a–c**, for which $\Delta R_{H\pi}$ is positive but almost negligible.

In all three-component complexes, the interaction energies are negative (see Table 1), with values that are larger than the sum of the interaction energies of the related CH/ π and Anion- π two-component systems. With the intention of analyzing the mutual influence between the Anion- π interaction and the CH/ π interaction, we have computed what we entitle the cooperativity energies (E_{coop} in Table 2) for complexes **8a–b**, **9a–d**, **10a–d**, and **11a–b**. The cooperativity energy is the result of subtracting the binding energies of geometry optimized two-component complexes and the binding energy of the interaction between the anion and methane as in **8–11** complexes from the binding energy of the three-component

complexes. For instance, in complex **9a** (methane⋯benzene⋯formate) we have computed the E_{coop} by subtracting the sum of three pair interaction energies: (i) benzene⋯formate (**4b**), (ii) methane⋯benzene (**2a**) and (iii) methane⋯formate as in **9a** from the binding energy of **9a**. This value gives important information regarding the interplay between both noncovalent interactions present in the complexes. It is worth mentioning that this term is negative in all complexes (it ranges from -0.37 to -0.54 kcal/mol, see Table 2), confirming the synergetic effects of both interactions, in agreement with the shortening of the equilibrium distances previously mentioned. The largest E_{coop} values are obtained for complexes **8** and **11** (-0.51 and -0.54 kcal/mol, respectively). However, E_{coop} is more important in complexes **9a** and **9b** because it amounts to 25.3% and 25.2%, respectively, of the total interaction energy (Table 2). In any case, it is worth noting that cooperativity energy values are remarkable because they represent between 17.6% and 25.3% ($\%E_{\text{coop}}$) of the total interaction energies. These results demonstrate that either the CH/ π interaction influences the Anion- π interaction or the Anion- π interaction influences the CH/ π interaction, or both.

Table 2. Cooperativity (E_{coop} , in kcal/mol), interaction energies of three-component complexes **8–11** computed as a two-component system ($E_{A\pi 2}$ and $E_{H\pi 2}$, in kcal/mol) and their relationship with their binary counterparts ($\Delta E_{A\pi} = E_{A\pi 2} - E_{A\pi 1}$ and $\Delta E_{H\pi} = E_{H\pi 2} - E_{H\pi 1}$), and weight of E_{coop} to the total interaction energy ($\%E_{\text{coop}}$) at the CCSD(T)/CBS//SCS-RI-MP2/AVTZ level of theory.

Compound	E_{coop}	$\%E_{\text{coop}}$	$E_{A\pi 2}$	$E_{H\pi 2}$	$\Delta E_{A\pi}$	$\Delta E_{H\pi}$
8a	-0.51	23.9	-0.66	-2.14	-0.68	-0.68
8b	-0.51	23.8	-0.67	-2.14	-0.68	-0.68
9a	-0.48	25.3	-0.53	-1.91	-0.55	-0.55
9b	-0.48	25.2	-0.54	-1.93	-0.55	-0.55
9c	-0.46	24.1	-0.53	-1.91	-0.54	-0.54
9d	-0.46	24.1	-0.52	-1.92	-0.54	-0.54
10a	-0.37	23.4	-0.36	-1.61	-0.38	-0.40
10b	-0.37	23.0	-0.39	-1.62	-0.40	-0.40
10c	-0.37	23.2	-0.39	-1.60	-0.39	-0.39
10d	-0.37	23.2	-0.38	-1.62	-0.40	-0.40
11a	-0.54	17.9	-1.56	-2.03	-0.57	-0.57
11b	-0.54	17.6	-1.58	-2.03	-0.56	-0.56

To further evaluate the effect of the Anion- π interaction on the CH/ π bonding and vice versa, we have computed the binding energy of the three-component complexes **8–11** using two different approaches (see Table 2 and Figure 3). First, we have computed the binding energies of complexes **8–11** considering that the CH/ π complex has been previously formed and evaluating the interaction with the anion as a two-component system ($A\pi 2$ with binding energy $E_{A\pi 2}$, for instance, **2a** + $\text{HCO}_2^- \rightarrow \text{9a}$). Second, we have computed the binding energies of complexes **8–11**, considering that the Anion- π complex has been previously formed and evaluating the interaction with methane as a two-component system ($H\pi 2$ with binding energy $E_{H\pi 2}$, for instance, **4a** + $\text{CH}_4 \rightarrow \text{9b}$). Finally, we have compared these binding energy values ($E_{A\pi 2}$ and $E_{H\pi 2}$) with the corresponding binding energies of the two-component complexes **1–7**, which we refer to as $E_{A\pi 1}$ and $E_{H\pi 1}$, present in Table 1. Therefore, we have also summarized in Table 2 the difference between the binding energies computed for the ternary complexes and the binding energies of the corresponding binary complexes (denoted as $\Delta E_{A\pi}$ and $\Delta E_{H\pi}$). The $\Delta E_{A\pi}$ and $\Delta E_{H\pi}$ values allow us to evaluate which noncovalent interaction is more strengthened in the ternary complexes with respect to the two-component complexes. Therefore, a negative value would mean that the interaction is strengthened, and a positive value would mean that the interaction is weakened in the three-component complex with respect to the corresponding two-component complex. The values of $\Delta E_{A\pi}$ and $\Delta E_{H\pi}$ computed for complexes **8–11** are negative in all cases, in agreement with the previously discussed energetic (E_{coop}) and geometric ($\Delta R_{H\pi}$ and $\Delta R_{A\pi}$) results. In fact, the largest $\Delta E_{H\pi}$ values correspond to the complexes with the largest $\Delta R_{H\pi}$ values (**8a–b** and **11a–b**). Therefore, both the Anion- π and CH/ π interactions are

reinforced with respect to their two-component counterparts when the benzene ring is interacting with methane on one side and with either formate or nitrate anion on the other side of the π system. Curiously, $\Delta E_{A\pi}$ and $\Delta E_{H\pi}$ have exactly the same values for each complex, and thus, according to these parameters, both interactions are equally reinforced on going from the two-component to the three-component complexes. All these interesting results allow us to learn which interaction in the multi-component system is reinforced. This information cannot be obtained from the cooperativity energies E_{coop} .

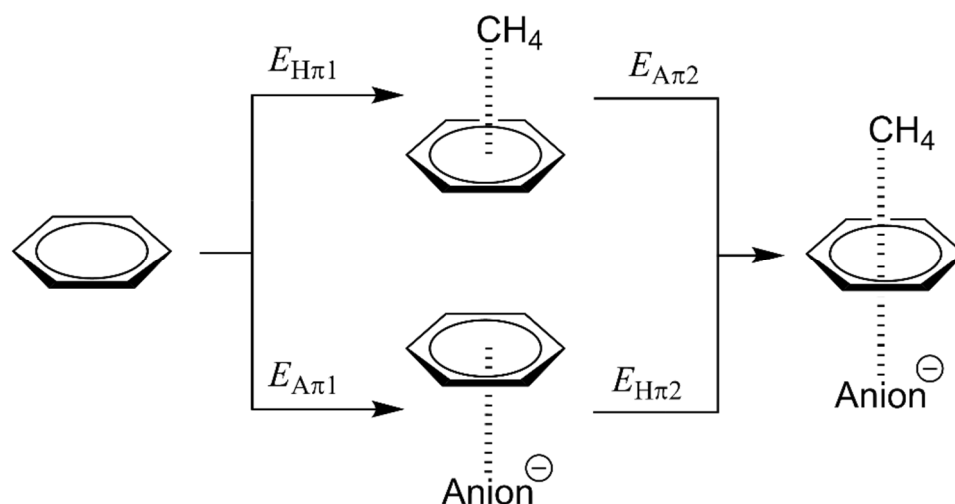


Figure 3. Schematic representation of the two routes to form the CH/ π -Anion complexes that allows computation of the $\Delta E_{H\pi}$ and $\Delta E_{A\pi}$ differences.

3.3. SAPT, AIM and NCI Analysis

To analyzing the electrostatic contribution of the Anion- π interaction and how it is affected by the formation of the CH/ π complex, we computed the electrostatic potential maps of benzene and complexes **1** and **2a** on their van der Waals surfaces. The computed ESP value on the center of the benzene molecule is -15.41 kcal/mol (Figure 4). For complex **1**, the computed ESP value on the side of the aromatic ring where methane is not located is -14.90 kcal/mol, i.e., on going from benzene to complex **1**, the ESP value on the benzene molecule becomes less negative by 0.51 kcal/mol and thus less repulsive if we would consider an Anion- π interaction on this side of the benzene molecular plane. Very similar results are obtained for complex **2a** (0.32 kcal/mol ESP difference). Therefore, as soon as the methane molecule begins to interact with benzene through CH/ π interactions as in complex **1**, the electron density of each molecule is polarized by the electric field of the other, resulting in a better Anion- π interaction on the free surface of the benzene molecule in complex **1**, than in free benzene.

These results urge us to expand the study and analysis of the physical nature of the interactions by carrying out SAPT calculations. The individual contributions to the interaction energy as obtained from the SAPT partitioning scheme are listed in Table 3 for selected complexes **1**, **2a**, **4b**, **9a**, **7b**, and **11b**. The values of the sum of all energy terms, E_{SAPT} , are close to the computed interaction energies at the CCSD(T) level of theory, as deduced from Table 3.

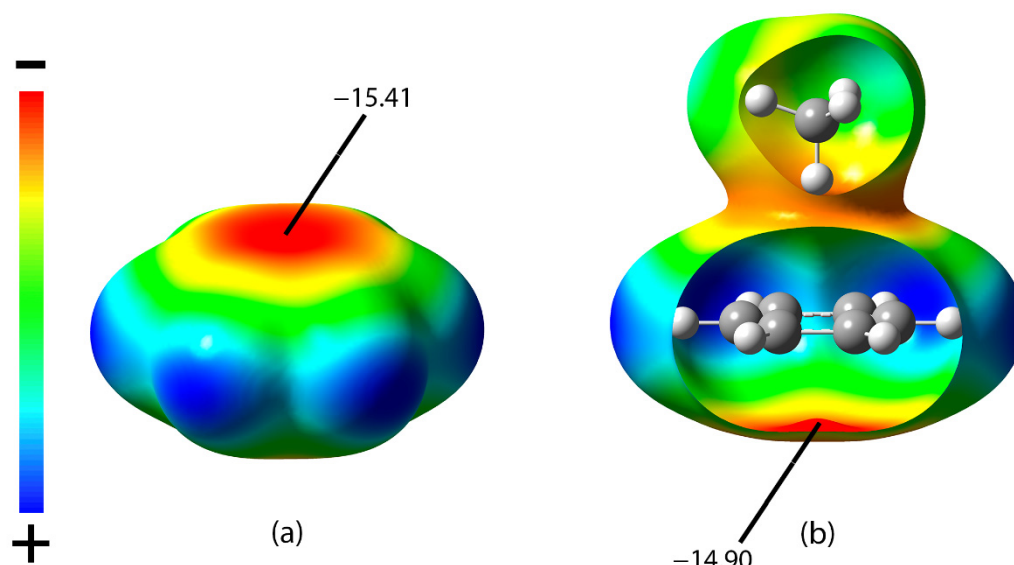


Figure 4. Electrostatic potential (ESP) on the 0.001 a.u. electron density isosurface of benzene (a), and complex **1** (b). The ESP energy values indicated are in kcal/mol. Carbon and hydrogen atoms are indicated in grey and white color, respectively.

Table 3. DF-DFT-symmetry-adapted perturbation theory (SAPT) electrostatic, exchange, induction, dispersion and Hartree-Fock higher-order energy contributions (E_{el} , E_{exch} , E_{ind} , E_{disp} and δHF , respectively), SAPT interaction energy (E_{SAPT}) and binding energies (E) of selected complexes. Energies in kcal/mol.

Compound	E_{el}	E_{ind}	E_{disp}	E_{exch}	δHF	E_{SAPT}	E	
1	−0.89	−0.10	−2.46	2.31	−0.17	−1.30	−1.46	
2a	−0.68	−0.07	−2.45	2.15	−0.15	−1.20	−1.37	
4b	3.75	−4.59	−3.85	4.84	0.01	0.16	0.02	
9a	H π 2	−0.99	−0.55	−2.77	2.75	−0.24	−1.81	−1.91
	A π 2	3.35	−4.94	−4.03	5.21	0.00	−0.40	−0.53
7b	H π 2	2.65	−3.22	−4.99	4.89	−0.18	−0.85	−0.99
	A π 2	−1.17	−0.50	−2.81	2.82	−0.27	−1.93	−2.03
11b	H π 2	−1.17	−0.50	−2.81	2.82	−0.27	−1.93	−2.03
	A π 2	2.19	−3.20	−5.21	5.26	−0.21	−1.17	−1.56

We first analyze the CH/ π interactions in complexes **1** and **2a**. We found that the electrostatic component (E_{el} in Table 3) is attractive for all the CH/ π complexes considered (**1** and **2a**, −0.89 and −0.68 kcal/mol, respectively). In these complexes, the induction term is very small, and the most important attractive contribution comes from dispersion effects (−2.46 and −2.45 kcal/mol) with a relative weight within all attractive forces of 65.7% and 71.2% for complexes **1** and **2a**, respectively. For the Anion- π complexes, the electrostatic term is repulsive (3.75 and 2.65 kcal/mol) as expected because of the large and negative quadrupole moment of benzene. For these complexes (**4b** and **7b**), the most important attractive contribution comes from E_{ind} and E_{disp} , respectively. Therefore, according to the SAPT calculations, the source of stabilization of the Anion- π stacking interaction in **7b**, compared to **4b**, is based on large dispersion effects (−4.99 kcal/mol) also keeping large induction effects (−3.22 kcal/mol) and a reduced electrostatic repulsive contribution.

To analyze the nature of the cooperativity effects in complexes **8–11**, we selected complexes **9a** and **11b** and computed the SAPT of three-component complexes using the approaches described in the previous section (see Figure 3). First, we computed the SAPT of **9a** and **11b**, considering that the Anion- π complex has been previously formed and examining the interaction with methane as a two-component system (e.g., **4b** + CH₄ → **9a**).

Second, we computed the SAPT of **9a** and **11b**, considering that the CH/ π complex has been previously formed and examining its interaction with the anion (e.g., **2a** + anion \rightarrow **9a**).

Let us first analyze the CH/ π interaction. For complexes **9a** and **11b**, all attractive contributions have been increased. For instance, the E_{el} , E_{ind} , and E_{disp} for the CH/ π interaction in **9a** have been increased by -0.31 , -0.48 , and -0.32 kcal/mol, respectively, with respect to complex **2a**. Similar results were obtained for complex **11b**. Despite dispersion being the major contributor to the CH/ π binding, with a relative weight of 61.2% and 59.2% for complexes **9a** and **11b**, respectively, the observed synergistic effects have their origin in the enhancement of all contributions, with a special mention on the induction term.

Let us continue with the analysis of the Anion- π interaction. For these complexes we observed that all energy contributions become more negative, except for the induction contribution in **11b**. As observed in complexes **4b** and **7b**, the major source of stabilization in **9a** and **11b** comes from induction and dispersion terms, respectively. It can be seen that the strengthening of the Anion- π interaction in **9a** is due primarily to an increase of all the attractive contributions, specifically the induction term (-0.35 kcal/mol) and a considerable decrease of the repulsive electrostatic term (-0.40 kcal/mol) on going from **4b** to **9a**. On the other hand, the observed strengthening in **11b** has a different nature since it comes primarily from a substantial reduction of the repulsive electrostatic contribution (-0.46 kcal/mol) and a slight increase in the dispersion term (-0.22 kcal/mol) on going from **7b** to **11b**.

Moreover, for all ternary complexes, the δ HF contribution always favours the interaction on going from two- to three-component complexes.

To further analyze the noncovalent character of these interactions, the AIM methodology was applied to assess the properties of the charge density for our systems. The molecular graphs of several two-component complexes are shown in Figure 5. The AIM analysis of the electron density in CH/ π complexes reveals the presence of two intermolecular bond critical points (BCP) that connect one (complex **1**), two H (complex **2a**), and three H atoms (complex **3a**) of methane with two (**1** and **2a**) and three C atoms (**3a**) of benzene (supplementary information, Figure S1). In addition, complexes **2b** and **3b** show two and three intermolecular BCP connecting methane with two and three intramolecular CC BCP of benzene, respectively. Analogously, very similar results are obtained for the Anion- π complexes (Figure 5 and Figure S1). For instance, the same number of BCP is obtained depending on the number of anion O atoms pointing at either C atoms or CC BCP of the aromatic ring. All intermolecular BCP is associated with the corresponding bond path connecting either H atoms of methane or O atoms of the anions with the benzene molecule. The values of the electron densities of BCP range between 0.0046 (complex **1**) and 0.0029 a.u. (complex **3b**) for CH/ π derivatives, and between 0.0047 (complexes **4a,b**) and 0.0035 a.u. (complex **5**) for Anion- π complexes (Table 4). Moreover, positive values of the Laplacian for all complexes were obtained, ranging between 0.0165 a.u. (complex **1**) and 0.0097 a.u. (complexes **3a,b**), and between 0.0152 (complexes **6a,b**) and 0.0135 (complex **5**) for CH/ π and Anion- π complexes, respectively, indicating close shell regime interactions. All these interactions are also characterized by the presence of one cage critical point (CCP). In Table 4 we gather the values of the electron density (ρ), and its Laplacian ($\nabla^2\rho$) computed at the cage critical points for complexes **1–7**. The molecular graphs of the three-component complexes are shown in Figure 6 and Figure S2. As can be observed, the distribution of the intermolecular BCP and CCP associated with both interactions is the same as the one obtained for the two-component complexes, except for complexes **11a,b**, where six BCP for the CH/ π interaction are located, as opposed to the two BCPs found in complex **1**. In Table S1, we also summarize the variation of the values of ρ and its Laplacian ($\nabla^2\rho$) in the complexes **8–11** with respect to the binary complexes **1–7** for the BCP and CCP. These values give information about the interplay between the noncovalent interaction involved in the complexes. It is worth remarking that the value of the charge density and its Laplacian computed at both BCP and CCP are greater in the three-component complexes than in the

two-component complexes, in agreement with the geometrical (shortening of equilibrium distances) and energetic results (E_{coop} values), thus confirming the synergetic effect of the simultaneous formation of the CH/ π and Anion- π interactions.

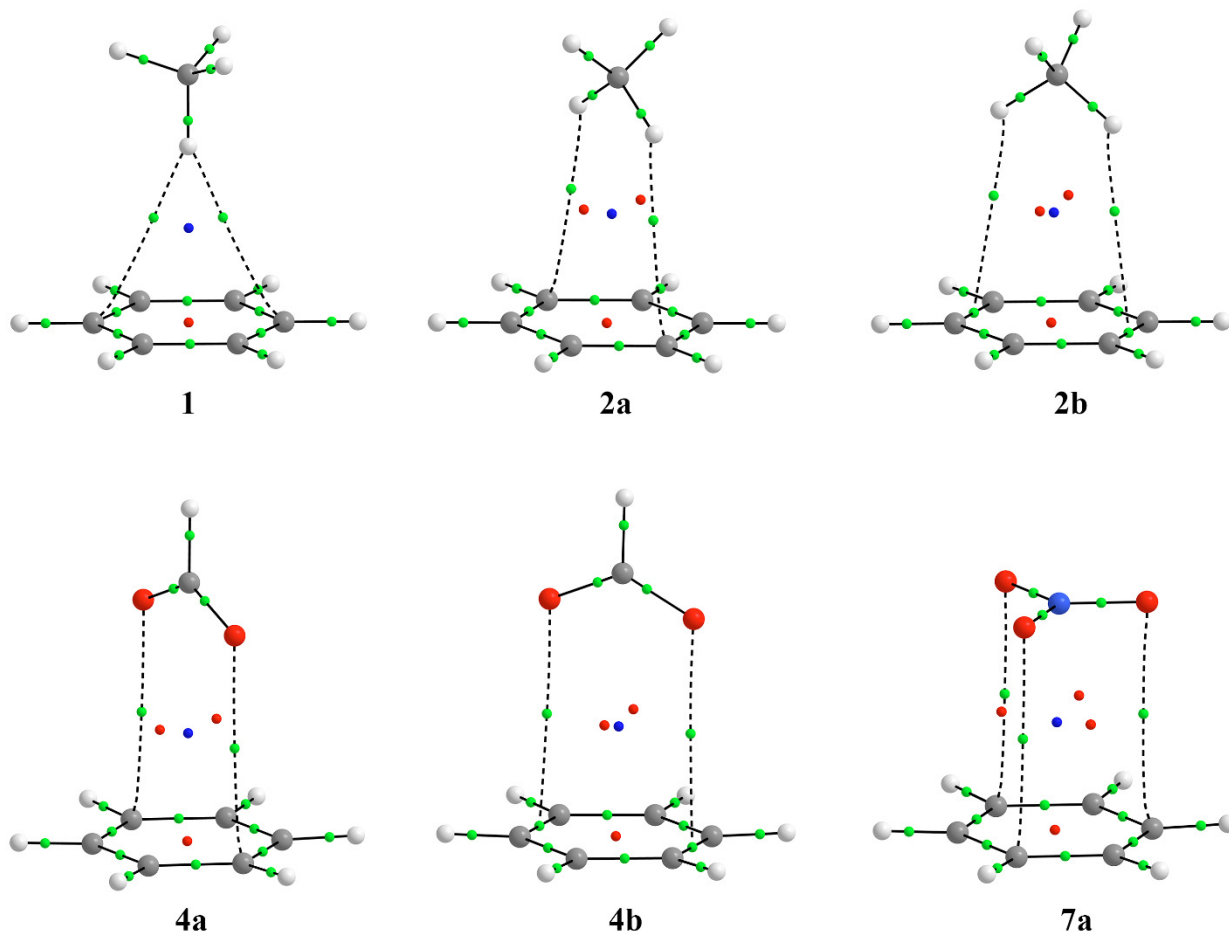


Figure 5. Molecular graphs of a selection of two-component complexes (**1**, **2a**, **2b**, **4a**, **4b**, **7a**). The BCPs, ring and cage critical points are represented by green, red, and blue dots, respectively. Only bond paths are depicted (intermolecular bond paths are shown as dashed lines). Carbon, nitrogen, oxygen, and hydrogen atoms are indicated in grey, blue, red, and white color, respectively.

Table 4. Electron density (ρ_{BCP} and ρ_{CCP}) and Laplacian ($\nabla^2\rho_{\text{BCP}}$ and $\nabla^2\rho_{\text{CCP}}$), in a.u., for the intermolecular bond critical points and cage critical points, respectively, in two-component complexes.

Compound	$\rho_{\text{BCP}} \times 10^3$	$\nabla^2\rho_{\text{BCP}} \times 10^2$	$\rho_{\text{CCP}} \times 10^3$	$\nabla^2\rho_{\text{CCP}} \times 10^2$
1	4.64	1.65	4.14	1.78
2a	3.93	1.24	2.44	1.07
2b	3.88	1.24	2.43	1.06
3a	2.98	0.97	2.02	0.89
3b	2.94	0.97	2.01	0.89
4a	4.73	1.46	2.13	0.86
4b	4.69	1.47	2.14	0.86
5	3.45	1.35	2.82	1.40
6a	4.61	1.52	2.11	0.92
6b	4.58	1.52	2.12	0.92
7a	4.61	1.50	2.27	1.14
7b	4.56	1.50	2.28	1.14

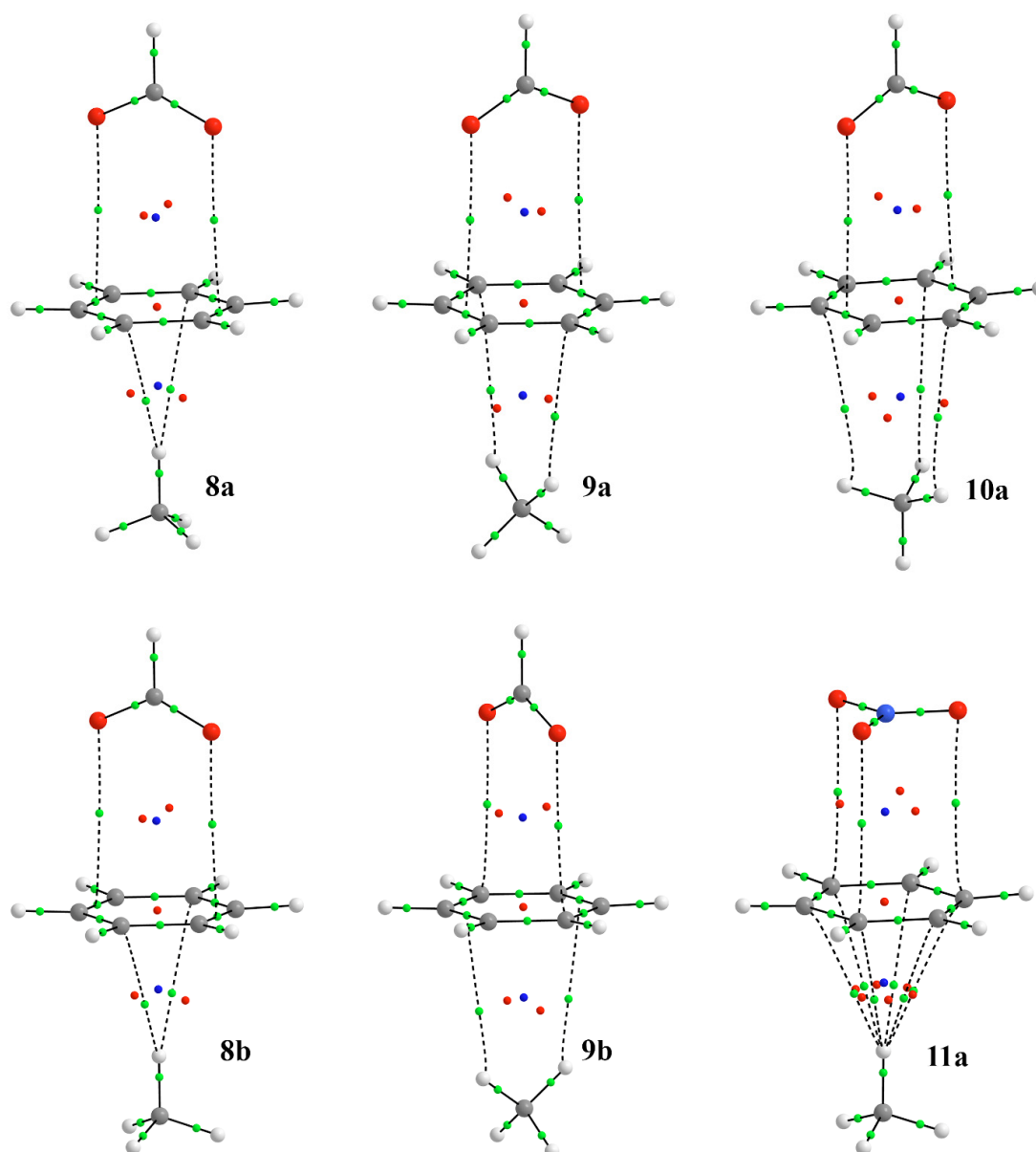


Figure 6. Molecular graphs of a selection of three-component complexes **8a**, **9a**, **10a**, **8b**, **9b**, **11a**. The BCPs, ring and cage critical points are represented by green, red, and blue dots, respectively. Only bond paths are depicted (intermolecular bond paths are shown as dashed lines). Carbon, nitrogen, oxygen, and hydrogen atoms are indicated in grey, blue, red, and white color, respectively.

Given that noncovalent interactions are characterized by low density (ρ) and reduced density gradient (RDG) values, they can be located using the NCIPLOT program [96]. These regions are mapped in real space by plotting an RDG isosurface for a low value of RDG, showing noncovalent interactions as broad regions of real space instead of simple pairwise contacts between atoms. Moreover, the sign of the second eigenvalue (λ_2) of the density Hessian times the density is color-mapped onto the isosurfaces. Moreover, the sign of λ_2 can be used to distinguish between bonded ($\lambda_2 < 0$) and non-bonded ($\lambda_2 > 0$) interactions, and, therefore, it can help to differentiate between different types of noncovalent interactions. The regions of very low density ($\rho < 0.005$ a.u.) correspond to weak dispersion interactions, while those of slightly higher density values ($0.005 < \rho < 0.05$ au) correspond to stronger noncovalent interactions [96]. Figure 7 shows the gradient isosurfaces for a selection of two- and three-component complexes (The gradient isosurfaces for the rest of the complexes are gathered in Figures S3–S5 of the Supplementary information). As can be observed,

there is an area of noncovalent interaction between the aromatic system and the methane molecule and the anion that covers the ring, just where the CH/ π and Anion- π interactions are expected. Similar gradient isosurfaces are obtained for the rest of the complexes. In Figure 7, the $\text{sign}(\lambda_2)\rho$ values obtained at the intersection between the isosurfaces and the AIM bond paths are included. In all cases, these values are <0 and correspond to the maxima of electron density for each interaction, confirming the nature of these bonding interactions. Moreover, for a given interaction, the ρ values are increased in the three-component complexes in relation to the two-component complexes, thus reinforcing the given interaction. For instance, the ρ value for the CH/ π interaction is increased from complex 2 (0.0040 au) to complex 9a (0.0044 au). Similarly, the density for the Anion- π interaction increases on going from complex 4 (0.0049 au) to complex 9a (0.0051 au). These results agree with previous results where we observe that the CH/ π interaction reinforces the Anion- π interaction and vice versa in the three-component complexes.

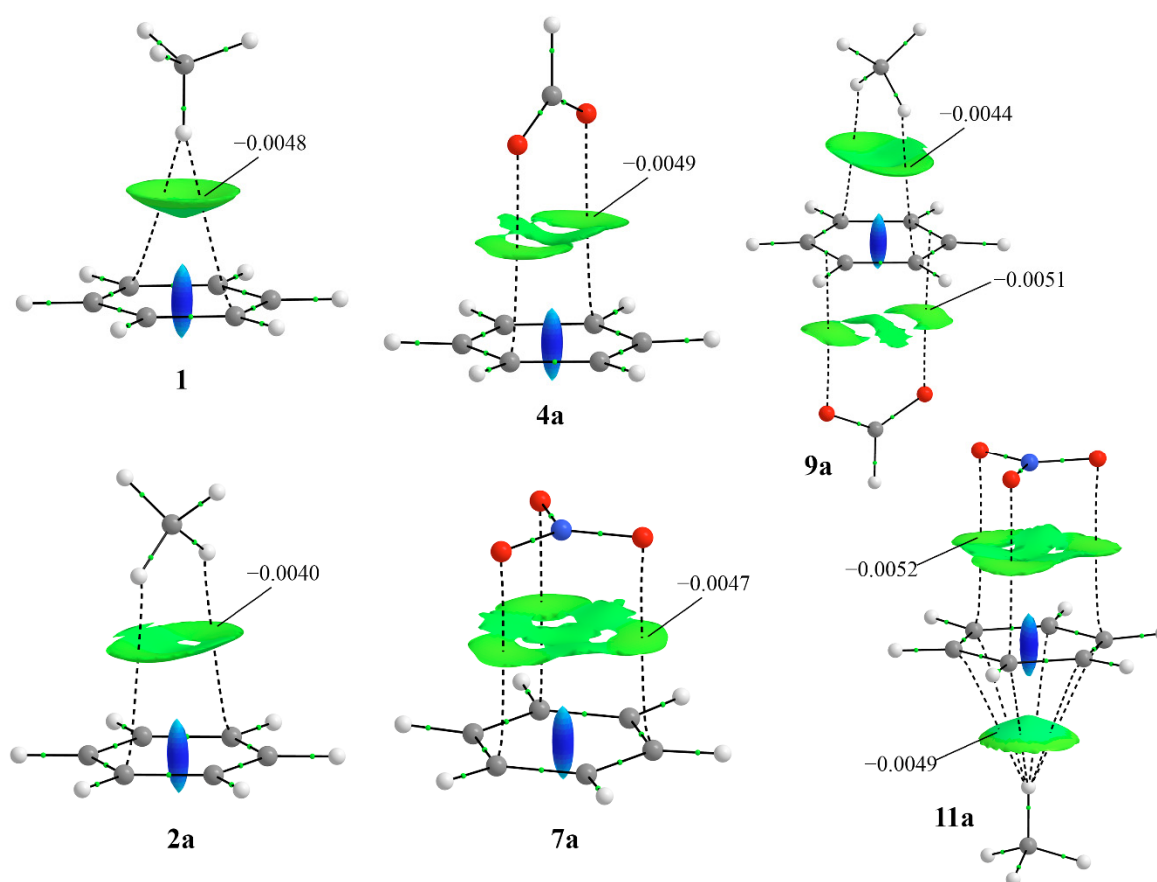


Figure 7. NCIPlot gradient isosurfaces (isovalue = 0.5 au) for CH/ π complexes **1** and **2a** (left), Anion- π complexes **4a** and **7a** (center), and three-component complexes **9a** and **11a** (right). Green and blue indicate weak and strongly repulsive interactions, respectively. Values of $\text{sign}(\lambda_2)\rho$ indicated are in au. Carbon, nitrogen, oxygen, and hydrogen atoms are indicated in grey, blue, red, and white color, respectively. Intermolecular bond paths are shown as dashed lines.

3.4. Experimental Evidences

Taking advantage of our previous study on Anion- π interactions in biomolecules [63], here we include two examples retrieved from the PDB in which Anion- π interactions with phenyl rings are operating concomitantly with CH/ π interactions coming from alkyl groups (Figure 8). In the first example, the authors report studies on the cellular protein cyclophilin A (CypA) and how it interacts with the HIV-1 capsid domain [99]. They found that the capsid sequence $^{87}\text{His-Ala-Gly-Pro-Ile-Ala}^{92}$ ($^{87}\text{HAGPIA}^{92}$) encompasses the primary cyclophilin A binding site, as shown in the reported X-ray crystal structure of the

CypA/HAGPIA complex. Although it was either not discussed or not noticed by the authors, the inspection of the structure reveals the presence of an Anion- π interaction between three carboxylate moiety of the C-terminal alanine of HAGPIA hexapeptide with the phenyl ring of phenylalanine 60 of CypA which, at the same time, is CH/ π interacting with a methylene group of methionine 61 of CypA (Figure 8, left).

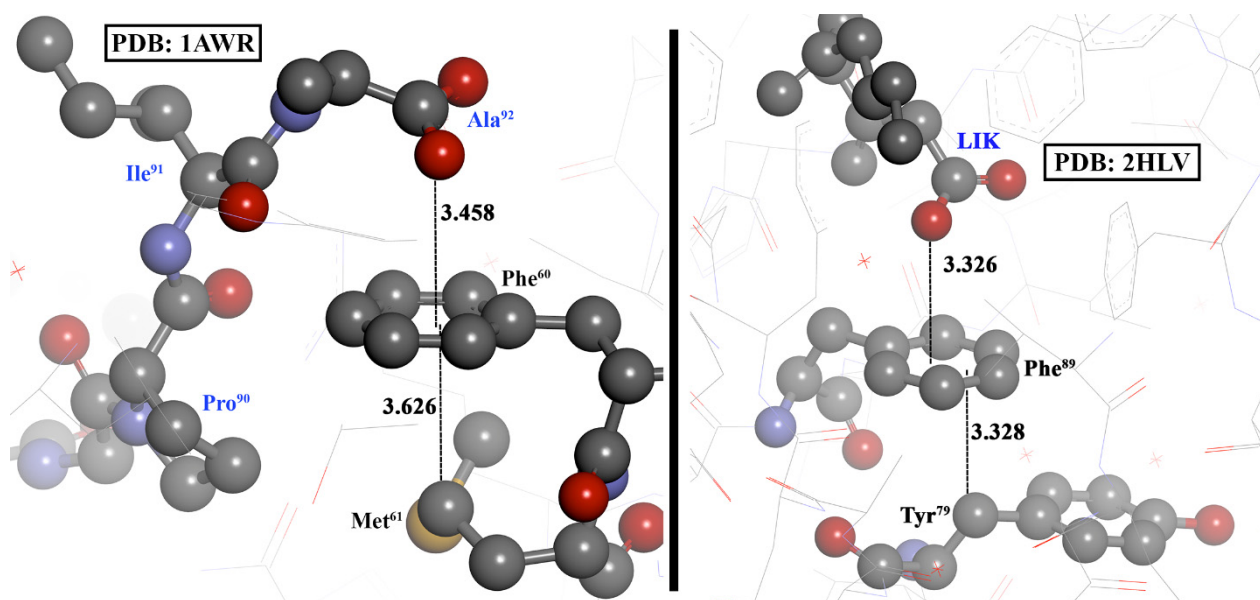


Figure 8. Partial views of X-ray structures of cellular protein cyclophilin A complexed with ⁸⁷HAGPIA⁹² peptide (left, PDB code 1AWR) and of triple mutant bovine Odorant Binding Protein complexed with 3,6-bis(methylene)decanoic acid, LIK (right, PDB code 2HLV). Distances to the ring plane are given in angstroms. Carbon, nitrogen, oxygen, and sulfur atoms are indicated in grey, blue, red, and yellow color, respectively (hydrogen have been omitted for clarity).

In the second example, the authors report a deswapping study of a mutant bovine Odorant Binding Protein (bOBP), describing its crystal structure and ligand binding properties, to decipher the evolutionary advantage of a domain swapping in native bOBP [100]. A partial view of the crystal structure of bOBP in a complex with 3,6-bis(methylene)decanoic acid (LIK) is shown in Figure 8. As can be seen, an unnoticed Anion- π interaction by the authors is established between the carboxylate group of the ligand and the aromatic ring of phenylalanine 89 of bOBP, which is simultaneously forming a CH/ π interaction on the opposite side of the aromatic ring with the conveniently located methylene group of tyrosine 79.

4. Conclusions

The results reported in this manuscript demonstrate the importance of the mutual influence between CH/ π and Anion- π interactions when the benzene molecule acts as the π -system, leading to strong synergetic effects. From the geometrical point of view, these effects are translated into a shortening of the equilibrium distances (0.02–0.05 Å) of both interactions on going from the two-component to the three-component complexes. From the energetics point of view, we obtained values of cooperativity energies E_{coop} ranging from -0.37 to -0.54 kcal/mol. These values are high since they represent between 17% and 25% of the total interaction energy, demonstrating that either the CH/ π interaction has an influence on the Anion- π interaction or the Anion- π interaction has an influence on the CH/ π interaction or both. By means of the approaches described in Figure 3, we have concluded that both Anion- π and CH/ π interactions are strengthened with respect to their two-component counterparts when the benzene ring is interacting with methane on one side and with an anion on another side of the π -system. All these interesting results

allow us to learn which interaction in the multi-component system is more reinforced, information that cannot be obtained from E_{coop} . Moreover, the SAPT energy partitioning scheme gives us valuable information on the origin of the observed synergetic effects. In this regard, the reinforcement of the CH/ π interaction has its origin in the enhancement of all contributions, with a special mention on the induction term, whereas the reinforcement of the Anion- π interaction is based on an increase of all attractive contributions coupled with a considerable decrease of the repulsive electrostatic term, except for the stacked complex **11b**, where the variation of the induction term is almost negligible. AIM and NCI results are also in agreement with the observed cooperativity effects and the strengthening of both interactions. Bearing in mind that many biomolecules and substrates contain phenyl groups, alkyl chains, and anionic groups, these synergetic effects might be crucial in different areas of biological chemistry.

Supplementary Materials: The following supporting information can be downloaded at: <https://www.mdpi.com/article/10.3390/sci4030032/s1>, Cartesian coordinates of all complexes; Figure S1: Molecular graphs of complexes **3a,b**, **5,6**, and **7b**. The BCPs, ring and cage critical points are represented by green, red, and blue dots, respectively. Only bond paths are depicted; Figure S2: Molecular graphs of complexes **9c,d**, **10b-d**, and **11b**. The BCPs, ring and cage critical points are represented by green, red, and blue dots, respectively. Only bond paths are depicted; Figure S3: NCIPLOT gradient isosurfaces (isovalue = 0.5 au) for two-component complexes **2b**, **3a,b**, **4b**, **5**, **6a,b**, and **7b**. Green and blue indicate weak and strongly repulsive interactions, respectively; Figure S4: NCIPLOT gradient isosurfaces (isovalue = 0.5 au) for three-component complexes **8a,b**, and **9b-d**. Green and blue indicate weak and strongly repulsive interactions, respectively; Figure S5: NCIPLOT gradient isosurfaces (isovalue = 0.5 au) for three-component complexes **10a-d**, and **11b**. Green and blue indicate weak and strongly repulsive interactions, respectively; Table S1: Variation of electron density ($\Delta\rho_{\text{BCP}}$ and $\Delta\rho_{\text{CCP}}$) and Laplacian ($\Delta\nabla^2\rho_{\text{BCP}}$ and $\Delta\nabla^2\rho_{\text{CCP}}$), in a.u., for the intermolecular bond critical points and cage critical points, respectively, in all three-component complexes with respect to the two-component analogues for the CH/ π (H π) and Anion- π (A π) interactions.

Author Contributions: Conceptualization, D.Q.; Investigation, D.Q.; Writing—original draft, D.Q.; Writing—review & editing, A.F. All authors have read and agreed to the published version of the manuscript.

Funding: This work was carried out with financial support from the project PID2020-115637GB-I00, FEDER FUNDS of the Ministerio de Ciencia, Innovación y Universidades of Spain.

Institutional Review Board Statement: Not applicable.

Informed Consent Statement: Not applicable.

Data Availability Statement: Not applicable.

Acknowledgments: We thank the CTI (UIB) for computational facilities.

Conflicts of Interest: The authors declare no conflict of interest.

References

1. Schneider, H.J. Binding Mechanisms in Supramolecular Complexes. *Angew. Chem. Int. Ed.* **2009**, *48*, 3924–3977. [[CrossRef](#)]
2. Quiñero, D.; Garau, C.; Rotger, C.; Frontera, A.; Ballester, P.; Costa, A.; Deyà, P.M. Anion- π Interactions: Do They Exist? *Angew. Chem. Int. Ed.* **2002**, *41*, 3389–3392. [[CrossRef](#)]
3. Mascal, M.; Armstrong, A.; Bartberger, M.D. Anion-Aromatic Bonding: A Case for Anion Recognition by π -Acidic Rings. *J. Am. Chem. Soc.* **2002**, *124*, 6274–6276. [[CrossRef](#)]
4. Alkorta, I.; Rozas, I.; Elguero, J. Interaction of Anions with Perfluoro Aromatic Compounds. *J. Am. Chem. Soc.* **2002**, *124*, 8593–8598. [[CrossRef](#)]
5. Quiñero, D.; Garau, C.; Frontera, A.; Ballester, P.; Costa, A.; Deyà, P.M. Counterintuitive interaction of anions with benzene derivatives. *Chem. Phys. Lett.* **2002**, *359*, 486–492. [[CrossRef](#)]
6. Ballester, P. Experimental Quantification of Anion- π Interactions in Solution Using Neutral Host-Guest Model Systems. *Acc. Chem. Res.* **2013**, *46*, 874–884. [[CrossRef](#)]
7. Kim, D.; Lee, E.C.; Kim, K.S.; Tarakeshwar, P. Cation- π -Anion Interaction: A Theoretical Investigation of the Role of Induction Energies. *J. Phys. Chem. A* **2007**, *111*, 7980–7986. [[CrossRef](#)]

8. Kim, D.; Tarakeshwar, P.; Kim, K.S. Theoretical Investigations of Anion- π Interactions: The Role of Anions and the Nature of π Systems. *J. Phys. Chem. A* **2004**, *108*, 1250–1258. [[CrossRef](#)]
9. Kim, D.Y.; Singh, N.J.; Kim, K.S. Cyameluric Acid as Anion- π Type Receptor for ClO_4^- and NO_3^- : π -Stacked and Edge-to-Face Structures. *J. Chem. Theory Comput.* **2008**, *4*, 1401–1407. [[CrossRef](#)]
10. Foroutan-Nejad, C.; Badri, Z.; Marek, R. Multi-center covalency: Revisiting the nature of Anion- π interactions. *Phys. Chem. Chem. Phys.* **2015**, *17*, 30670–30679. [[CrossRef](#)]
11. Novák, M.; Foroutan-Nejad, C.; Marek, R. Modulating Electron Sharing in Ion- π -Receptors via Substitution and External Electric Field: A Route toward Bond Strengthening. *J. Chem. Theory Comput.* **2016**, *12*, 3788–3795. [[CrossRef](#)] [[PubMed](#)]
12. Schottel, B.L.; Chifotides, H.T.; Dunbar, K.R. Anion- π interactions. *Chem. Soc. Rev.* **2008**, *37*, 68–83. [[CrossRef](#)] [[PubMed](#)]
13. Gamez, P.; Mooibroek, T.J.; Teat, S.J.; Reedijk, J. Anion Binding Involving π -Acidic Heteroaromatic Rings. *Acc. Chem. Res.* **2007**, *40*, 435–444. [[CrossRef](#)]
14. Frontera, A.; Gamez, P.; Mascal, M.; Mooibroek, T.J.; Reedijk, J. Putting Anion- π Interactions into Perspective. *Angew. Chem. Int. Ed.* **2011**, *50*, 9564–9583. [[CrossRef](#)]
15. Garau, C.; Frontera, A.; Quiñonero, D.; Ballester, P.; Costa, A.; Deyà, P.M. Anion- π Interactions. *Recent Res. Dev. Chem. Phys.* **2004**, *5*, 227–255. [[CrossRef](#)]
16. Chifotides, H.T.; Dunbar, K.R. Anion- π Interactions in Supramolecular Architectures. *Acc. Chem. Res.* **2013**, *46*, 894–906. [[CrossRef](#)] [[PubMed](#)]
17. Wang, D.-X.; Wang, M.-X. Exploring Anion- π Interactions and Their Applications in Supramolecular Chemistry. *Acc. Chem. Res.* **2020**, *53*, 1364–1380. [[CrossRef](#)] [[PubMed](#)]
18. Rather, I.A.; Wagay, S.A.; Ali, R. Emergence of anion- π interactions: The land of opportunity in supramolecular chemistry and beyond. *Coord. Chem. Rev.* **2020**, *415*, 213327. [[CrossRef](#)]
19. Zhuang, S.-Y.; Cheng, Y.; Zhang, Q.; Tong, S.; Wang, M.-X. Synthesis of *i*-Corona[6]arenes for Selective Anion Binding: Interdependent and Synergistic Anion- π and Hydrogen-Bond Interactions. *Angew. Chem. Int. Ed.* **2020**, *59*, 23716–23723. [[CrossRef](#)]
20. Gong, H.; Zhang, C.; Ogaki, T.; Inuzuka, H.; Hashizume, D.; Miyajima, D. Azacalix[3]triazines: A Substructure of Triazine-Based Graphitic Carbon Nitride Featuring Anion- π Interactions. *Angew. Chem. Int. Ed.* **2021**, *60*, 16377–16381. [[CrossRef](#)]
21. Maynard, J.R.J.; Galmés, B.; Stergiou, A.D.; Symes, M.D.; Frontera, A.; Goldup, S.M. Anion- π Catalysis Enabled by the Mechanical Bond. *Angew. Chem. Int. Ed.* **2022**, *61*, e202115961. [[CrossRef](#)]
22. Clements, A.; Lewis, M. Arene-Cation Interactions of Positive Quadrupole Moment Aromatics and Arene-Anion Interactions of Negative Quadrupole Moment Aromatics. *J. Phys. Chem. A* **2006**, *110*, 12705–12710. [[CrossRef](#)]
23. Geronimo, I.; Singh, N.J.; Kim, K.S. Can Electron-Rich π Systems Bind Anions? *J. Chem. Theory Comput.* **2011**, *7*, 825–829. [[CrossRef](#)]
24. Elgengehi, S.M.; El-Taher, S.; Ibrahim, M.A.A.; El-Kelany, K.E. Unexpected favourable noncovalent interaction between chlorine oxyanions (ClO_x^- ; $x = 1-4$) and benzene: Benchmarking DFT and SAPT methods with respect to CCSD(T). *Comput. Theor. Chem.* **2021**, *1199*, 113214. [[CrossRef](#)]
25. Xu, Z.; Singh, N.J.; Kim, S.K.; Spring, D.R.; Kim, K.S.; Yoon, J. Induction-Driven Stabilization of the Anion- π Interaction in Electron-Rich Aromatics as the Key to Fluoride Inclusion in Imidazolium-Cage Receptors. *Chem. Eur. J.* **2011**, *17*, 1163–1170. [[CrossRef](#)]
26. Estarellas, C.; Frontera, A.; Quiñonero, D.; Deyà, P.M. Relevant Anion- π Interactions in Biological Systems: The Case of Urate Oxidase. *Angew. Chem. Int. Ed.* **2011**, *50*, 415–418. [[CrossRef](#)]
27. Robertazzi, A.; Krull, F.; Knapp, E.-W.; Gamez, P. Recent advances in Anion- π interactions. *CrystEngComm* **2011**, *13*, 3293–3300. [[CrossRef](#)]
28. Estarellas, C.; Frontera, A.; Quiñonero, D.; Deyà, P.M. Anion- π Interactions in Flavoproteins. *Chem. Asian J.* **2011**, *6*, 2316–2318. [[CrossRef](#)]
29. Philip, V.; Harris, J.; Adams, R.; Nguyen, D.; Baudry, J.; Howell, E.E.; Hinde, R.J. A Survey of Aspartate-Phenylalanine and Glutamate-Phenylalanine Interactions in the Protein Data Bank: Searching for Anion- π Pairs. *Biochemistry* **2011**, *50*, 2939–2950. [[CrossRef](#)]
30. Chakravarty, S.; Sheng, Z.-Z.; Iverson, B.; Moore, B. “ η^6 ”-Type Anion- π in biomolecular recognition. *FEBS Lett.* **2012**, *586*, 4180–4185. [[CrossRef](#)]
31. Breberina, L.M.; Milčić, M.K.; Nikolić, M.R.; Stojanović, S.Đ. Contribution of Anion- π interactions to the stability of Sm/LSM proteins. *JBC J. Biol. Inorg. Chem.* **2014**, *20*, 475–485. [[CrossRef](#)] [[PubMed](#)]
32. Bauzá, A.; Quiñonero, D.; Deyà, P.M.; Frontera, A. On the Importance of Anion- π Interactions in the Mechanism of Sulfide: Quinone Oxidoreductase. *Chem. Asian J.* **2013**, *8*, 2708–2713. [[CrossRef](#)] [[PubMed](#)]
33. Bauzá, A.; Quiñonero, D.; Deyà, P.M.; Frontera, A. Long-Range Effects in Anion- π Interactions: Their Crucial Role in the Inhibition Mechanism of Mycobacterium Tuberculosis Malate Synthase. *Chem. Eur. J.* **2014**, *20*, 6985–6990. [[CrossRef](#)]
34. Jenkins, D.D.; Harris, J.B.; Howell, E.E.; Hinde, R.; Baudry, J. STAAR: Statistical analysis of aromatic rings. *J. Comput. Chem.* **2013**, *34*, 518–522. [[CrossRef](#)] [[PubMed](#)]
35. Smith, M.S.; Lawrence, E.E.K.; Billings, W.M.; Larsen, K.S.; Bécar, N.A.; Price, J.L. An Anion- π Interaction Strongly Stabilizes the β -Sheet Protein WW. *ACS Chem. Biol.* **2017**, *12*, 2535–2537. [[CrossRef](#)]
36. Nishio, M. CH/ π hydrogen bonds in crystals. *CrystEngComm* **2004**, *6*, 130–158. [[CrossRef](#)]

37. Takahashi, O.; Kohno, Y.; Nishio, M. Relevance of Weak Hydrogen Bonds in the Conformation of Organic Compounds and Bioconjugates: Evidence from Recent Experimental Data and High-Level ab Initio MO Calculations. *Chem. Rev.* **2010**, *110*, 6049–6076. [[CrossRef](#)]
38. Salonen, L.M.; Ellermann, M.; Diederich, F. Aromatic Rings in Chemical and Biological Recognition: Energetics and Structures. *Angew. Chem. Int. Ed.* **2011**, *50*, 4808–4842. [[CrossRef](#)]
39. Tsuzuki, S.; Fujii, A. Nature and physical origin of CH/ π interaction: Significant difference from conventional hydrogen bonds. *Phys. Chem. Chem. Phys.* **2008**, *10*, 2584–2594. [[CrossRef](#)]
40. Nishio, M.; Umezawa, Y.; Honda, K.; Tsuboyama, S.; Suezawa, H. CH/ π hydrogen bonds in organic and organometallic chemistry. *CrystEngComm* **2009**, *11*, 1757–1788. [[CrossRef](#)]
41. Nishio, M.; Hirota, M. CH/ π interaction: Implications in organic chemistry. *Tetrahedron* **1989**, *45*, 7201–7245. [[CrossRef](#)]
42. Nishio, M.; Umezawa, Y. The CH/Hydrogen Bond: An Important Molecular Force in Controlling the Crystal Conformation of Organic Compounds and Three-Dimensional Structure of Biopolymers. *Top Stereochem.* **2006**, *25*, 255–307.
43. Nishio, M.; Hirota, M.; Umezawa, Y. *The CH/ π Interaction: Evidence, Nature, and Consequences*; Wiley-VCH: New York, NY, USA, 1998.
44. Nishio, M. CH/ π hydrogen bonds in organic reactions. *Tetrahedron* **2005**, *61*, 6923–6950. [[CrossRef](#)]
45. Klein, E.; Ferrand, Y.; Barwell, N.P.; Davis, A.P. Solvent Effects in Carbohydrate Binding by Synthetic Receptors: Implications for the Role of Water in Natural Carbohydrate Recognition. *Angew. Chem. Int. Ed.* **2008**, *47*, 2693–2696. [[CrossRef](#)] [[PubMed](#)]
46. Ferrand, Y.; Crump, M.P.; Davis, A.P. A Synthetic Lectin Analog for Biomimetic Disaccharide Recognition. *Science* **2007**, *318*, 619–622. [[CrossRef](#)] [[PubMed](#)]
47. Trembleau, L.; Rebek, J., Jr. Helical Conformation of Alkanes in a Hydrophobic Cavitand. *Science* **2003**, *301*, 1219–1220. [[CrossRef](#)]
48. Hooley, R.J.; Van Anda, H.J.; Rebek, J., Jr. Extraction of Hydrophobic Species into a Water-Soluble Synthetic Receptor. *J. Am. Chem. Soc.* **2007**, *129*, 13464–13473. [[CrossRef](#)]
49. Scarso, A.; Trembleau, L.; Rebek, J., Jr. Encapsulation Induces Helical Folding of Alkanes. *Angew. Chem. Int. Ed.* **2003**, *42*, 5499–5502. [[CrossRef](#)]
50. Scarso, A.; Trembleau, L.; Rebek, J., Jr. Helical Folding of Alkanes in a Self-Assembled, Cylindrical Capsule. *J. Am. Chem. Soc.* **2004**, *126*, 13512–13518. [[CrossRef](#)]
51. Carrillo, R.; López-Rodríguez, M.; Martín, V.S.; Martín, T. Quantification of a CH- π Interaction Responsible for Chiral Discrimination and Evaluation of Its Contribution to Enantioselectivity. *Angew. Chem. Int. Ed.* **2009**, *48*, 7803–7808. [[CrossRef](#)]
52. Ballester, P.; Capó, M.; Costa, A.; Deyà, P.M.; Gomila, R.; Decken, A.; Deslongchamps, G. Dual Binding Mode of Methylmethane-triacetic Acid to Tripodal Amidopyridine Receptors. *J. Org. Chem.* **2002**, *67*, 8832–8841. [[CrossRef](#)] [[PubMed](#)]
53. Frontera, A.; Garau, C.; Quiñonero, D.; Ballester, P.; Costa, A.; Deyà, P.M. Weak C-H/ π Interaction Participates in the Diastereoselectivity of a Host-Guest Complex in the Presence of Six Strong Hydrogen Bonds. *Org. Lett.* **2003**, *5*, 1135–1138. [[CrossRef](#)] [[PubMed](#)]
54. Shibusaki, K.; Fujii, A.; Mikami, N.; Tsuzuki, S. Magnitude and Nature of Interactions in Benzene-X (X = Ethylene and Acetylene) in the Gas Phase: Significantly Different CH/ π Interaction of Acetylene as Compared with Those of Ethylene and Methane. *J. Phys. Chem. A* **2007**, *111*, 753–758. [[CrossRef](#)]
55. Ringer, A.L.; Figgs, M.S.; Sinnokrot, M.O.; Sherrill, C.D. Aliphatic C-H/ π Interactions: Methane-Benzene, Methane-Phenol, and Methane-Indole Complexes. *J. Phys. Chem. A* **2006**, *110*, 10822–10828. [[CrossRef](#)] [[PubMed](#)]
56. Stone, A.J. Computation of charge-transfer energies by perturbation theory. *Chem. Phys. Lett.* **1993**, *211*, 101–109. [[CrossRef](#)]
57. Nishio, M.; Umezawa, Y.; Fantini, J.; Weiss, M.S.; Chakrabarti, P. CH- π hydrogen bonds in biological macromolecules. *Phys. Chem. Chem. Phys.* **2014**, *16*, 12648–12683. [[CrossRef](#)] [[PubMed](#)]
58. Umezawa, Y.; Nishio, M. CH/ π Interactions as demonstrated in the crystal structure of guanine-nucleotide binding proteins, Src homology-2 domains and human growth hormone in complex with their specific ligands. *Bioorg. Med. Chem.* **1998**, *6*, 493–504. [[CrossRef](#)]
59. Tatko, C.D.; Waters, M.L. Comparison of C-H \cdots π and Hydrophobic Interactions in a β -Hairpin Peptide: Impact on Stability and Specificity. *J. Am. Chem. Soc.* **2004**, *126*, 2028–2034. [[CrossRef](#)]
60. Umezawa, Y.; Nishio, M. CH/ π interactions in the crystal structure of class I MHC antigens and their complexes with peptides. *Bioorg. Med. Chem.* **1998**, *6*, 2507–2515. [[CrossRef](#)]
61. Umezawa, Y.; Nishio, M. CH/ π interactions in the crystal structure of TATA₁ box binding protein/DNA complexes. *Bioorg. Med. Chem.* **2000**, *8*, 2643–2650. [[CrossRef](#)]
62. Spiwok, V. CH/ π Interactions in Carbohydrate Recognition. *Molecules* **2017**, *22*, 1038. [[CrossRef](#)] [[PubMed](#)]
63. Lucas, X.; Bauzá, A.; Frontera, A.; Quiñonero, D. A thorough Anion- π interaction study in biomolecules: On the importance of cooperativity effects. *Chem. Sci.* **2016**, *7*, 1038–1050. [[CrossRef](#)] [[PubMed](#)]
64. Quiñonero, D.; Frontera, A.; Garau, C.; Ballester, P.; Costa, A.; Deyà, P.M. Interplay between cation- π , Anion- π and π - π interactions. *Chem. Phys. Chem.* **2006**, *7*, 2487–2491. [[CrossRef](#)] [[PubMed](#)]
65. Frontera, A.; Quiñonero, D.; Costa, A.; Ballester, P.; Deyà, P.M. MP2 study of cooperative effects between cation- π , anion- π and π - π interactions. *New J. Chem.* **2007**, *31*, 556–560. [[CrossRef](#)]
66. Lucas, X.; Estarellas, C.; Escudero, D.; Frontera, A.; Quiñonero, D.; Deyà, P.M. Very long-range effects: Cooperativity between Anion- π and hydrogen-bonding interactions. *ChemPhysChem* **2009**, *10*, 2256–2264. [[CrossRef](#)]

67. Escudero, D.; Frontera, A.; Quiñonero, D.; Deyà, P.M. Interplay between Anion- π and hydrogen-bonding interactions. *J. Comput. Chem.* **2009**, *30*, 75–82. [CrossRef]
68. Ebrahimi, A.; Masoodi, H.R.; Khorassani, M.H.; Ghaleno, M.H. The influence of cation- π and Anion- π interactions on the strength and nature of N-H hydrogen bond. *Comput. Theor. Chem.* **2012**, *988*, 48–55. [CrossRef]
69. Azizi, A.; Ebrahimi, A. The X \cdots benzohydrazide complexes: The interplay between anion- π and H-bond interactions. *Struct. Chem.* **2016**, *28*, 687–695. [CrossRef]
70. Quiñonero, D.; Frontera, A.; Deyà, P.M. Interplay between ion- π and Ar/ π Van der Waals interactions. *Comput. Theor. Chem.* **2012**, *998*, 51–56. [CrossRef]
71. Estarellas, C.; Frontera, A.; Quiñonero, D.; Deyà, P.M. Theoretical study on cooperativity effects between Anion- π and halogen-bonding interactions. *ChemPhysChem* **2011**, *12*, 2742–2750. [CrossRef]
72. Razmazma, H.; Ebrahimi, A. The effects of cation- π and Anion- π interactions on halogen bonds in the [N \cdots X \cdots N]⁺ complexes: A comprehensive theoretical study. *J. Mol. Graph. Model.* **2018**, *84*, 134–144. [CrossRef]
73. Du, S.; Wang, B.; Zhang, J.; Zhang, C. Tuning anion- π interaction via halogen substituent effects in cyanuric acids and its derivatives. *Int. J. Quantum Chem.* **2015**, *115*, 1147–1152. [CrossRef]
74. Esrafil, M.D.; Mousavian, P. The triel bond: A potential force for tuning Anion- π interactions. *Mol. Phys.* **2018**, *116*, 388–398. [CrossRef]
75. Feyereisen, M.W.; Fitzgerald, G.; Komornicki, A. Use of approximate integrals in ab initio theory. An application in MP2 energy calculations. *Chem. Phys. Lett.* **1993**, *208*, 359–363. [CrossRef]
76. Vahtras, O.; Almlöf, J.; Feyereisen, M.W. Integral approximations for LCAO-SCF calculations. *Chem. Phys. Lett.* **1993**, *213*, 514–518. [CrossRef]
77. Grimme, S. Improved second-order Møller–Plesset perturbation theory by separate scaling of parallel- and antiparallel-spin pair correlation energies. *J. Chem. Phys.* **2003**, *118*, 9095–9102. [CrossRef]
78. Grimme, S.; Goerigk, L.; Fink, R.F. Spin-component-scaled electron correlation methods. *WIREs Comput. Mol. Sci.* **2012**, *2*, 886–906. [CrossRef]
79. Gerenkamp, M.; Grimme, S. Spin-component scaled second-order Møller–Plesset perturbation theory for the calculation of molecular geometries and harmonic vibrational frequencies. *Chem. Phys. Lett.* **2004**, *392*, 229–235. [CrossRef]
80. Quiñonero, D.; Frontera, A. Hydrogen Bond versus Halogen Bond in HXO_n (X = F, Cl, Br, and I) Complexes with Lewis Bases. *Inorganics* **2019**, *7*, 9. [CrossRef]
81. Halkier, A.; Helgaker, T.; Jørgensen, P.; Klopper, W.; Olsen, J. Basis-set convergence of the energy in molecular Hartree–Fock calculations. *Chem. Phys. Lett.* **1999**, *302*, 437–446. [CrossRef]
82. Halkier, A.; Klopper, W.; Helgaker, T.; Jørgensen, P.; Taylor, P.R. Basis set convergence of the interaction energy of hydrogen-bonded complexes. *J. Chem. Phys.* **1999**, *111*, 9157–9167. [CrossRef]
83. TURBOMOLE V7.0 2015, a Development of University of Karlsruhe and Forschungszentrum Karlsruhe GmbH, 1989–2007, TURBOMOLE GmbH, Since 2007. Available online: <http://www.turbomole.com> (accessed on 10 May 2022).
84. Werner, H.-J.; Knowles, P.J.; Manby, F.R.; Schütz, M.; Celani, P.; Knizia, G.; Korona, T.; Lindh, R.; Mitrushenkov, A.; Rauhut, G.; et al. *MOLPRO*, Version 2010.1. A Package of ab Initio Programs. Stuttgart, Germany.
85. Bader, R.F.W. *Atoms in Molecules: A Quantum Theory*; Clarendon Press: Oxford, UK, 1990.
86. Popelier, P.L.A. *Atoms in Molecules: An Introduction*; Prentice Hall: Harlow, UK, 2000.
87. Keith, T.A. *TK Gristmill Software*, version 19.10.12 edn. Overland Park, KS, USA; 2019. Available online: aim.tkgristmill.com (accessed on 26 April 2022).
88. Jeziorski, B.; Moszynski, R.; Szalewicz, K. Perturbation Theory Approach to Intermolecular Potential Energy Surfaces of van der Waals Complexes. *Chem. Rev.* **1994**, *94*, 1887–1930. [CrossRef]
89. Quiñonero, D. Anion Recognition by Pyrylium Cations and Thio-, Seleno- and Telluro- Analogues: A Combined Theoretical and Cambridge Structural Database Study. *Molecules* **2015**, *20*, 11632–11659. [CrossRef]
90. Misquitta, A.J.; Podeszwa, R.; Jeziorski, B.; Szalewicz, K. Intermolecular potentials based on symmetry-adapted perturbation theory with dispersion energies from time-dependent density-functional calculations. *J. Chem. Phys.* **2005**, *123*, 214103–214114. [CrossRef]
91. Hesselmann, A.; Jansen, G. The helium dimer potential from a combined density functional theory and symmetry-adapted perturbation theory approach using an exact exchange–correlation potential. *Phys. Chem. Chem. Phys.* **2003**, *5*, 5010–5014. [CrossRef]
92. Moszynski, R. Symmetry-adapted perturbation theory for the calculation of Hartree-Fock interaction energies. *Mol. Phys.* **1996**, *88*, 741–758.
93. Perdew, J.P.; Burke, K.; Ernzerhof, M. Generalized Gradient Approximation Made Simple. *Phys. Rev. Lett.* **1996**, *77*, 3865–3868. [CrossRef]
94. Weigend, F. A fully direct RI-HF algorithm: Implementation, optimised auxiliary basis sets, demonstration of accuracy and efficiency. *Phys. Chem. Chem. Phys.* **2002**, *4*, 4285–4291. [CrossRef]
95. Weigend, F.; Köhn, A.; Hättig, C. Efficient use of the correlation consistent basis sets in resolution of the identity MP2 calculations. *J. Chem. Phys.* **2002**, *116*, 3175–3183. [CrossRef]

96. Johnson, E.R.; Keinan, S.; Mori-Sánchez, P.; Contreras-García, J.; Cohen, A.J.; Yang, W. Revealing noncovalent interactions. *J. Am. Chem. Soc.* **2010**, *132*, 6498–6506. [[CrossRef](#)]
97. Tsuzuki, S.; Honda, K.; Uchimaru, T.; Mikami, M.; Fujii, A. Magnitude and Directionality of the Interaction Energy of the Aliphatic CH/ π Interaction: Significant Difference from Hydrogen Bond. *J. Phys. Chem. A* **2006**, *110*, 10163–10168. [[CrossRef](#)]
98. Bauzá, A.; Frontera, A.; Mooibroek, T. NO₃[−] anions can act as Lewis acid in the solid state. *Nat. Commun.* **2017**, *8*, 14522. [[CrossRef](#)]
99. Vajdos, F.F.; Yoo, S.; Houseweart, M.; Sundquist, W.I.; Hill, C.P. Crystal structure of cyclophilin A complexed with a binding site peptide from the HIV-1 capsid protein. *Protein Sci.* **1997**, *6*, 2297–2307. [[CrossRef](#)]
100. Ramoni, R.; Spinelli, S.; Grolli, S.; Conti, V.; Merli, E.; Cambillau, C.; Tegoni, M. Deswapping bovine odorant binding protein. *Biochim. Biophys. Acta* **2008**, *1784*, 651–657. [[CrossRef](#)]